

Response of Soft Continuous Structures and Topological Defects to a Temperature Gradient

Rei Kurita,^{1,2,*} Shun Mitsui,¹ and Hajime Tanaka^{2,†}

¹*Department of Physics, Tokyo Metropolitan University, 1-1 Minami-Osawa, Hachioji-City, Tokyo 192-0397, Japan*

²*Department of Fundamental Engineering, Institute of Industrial Science, University of Tokyo, 4-6-1 Komaba, Meguro-ku, Tokyo 153-8505, Japan*

(Received 19 November 2016; revised manuscript received 24 March 2017; published 8 September 2017)

Thermophoresis, which is mass transport induced by a temperature gradient, has recently attracted considerable attention as a new way to transport materials. So far the study has been focused on the transport of discrete structures such as colloidal particles, proteins, and polymers in solutions. However, the response of soft continuous structures such as membranes and gels to a temperature gradient has been largely unexplored. Here we study the behavior of a lamellar phase made of stacked surfactant bilayer membranes under a temperature gradient. We find the migration of membranes towards a low-temperature region, causing the increase in the degree of membrane undulation fluctuations towards that direction. This is contrary to our intuition that the fluctuations are weaker at a lower temperature. We show that this can be explained by temperature-gradient-induced migration of membranes under the topological constraint coming from the connectivity of each membrane. We also reveal that the pattern of an edge dislocation array formed in a wedge-shaped cell can be controlled by a temperature gradient. These findings suggest that application of a temperature gradient provides a novel way to control the organization of soft continuous structures such as membranes, gels, and foams, in a manner essentially different from the other types of fields, and to manipulate topological defects.

DOI: [10.1103/PhysRevLett.119.108003](https://doi.org/10.1103/PhysRevLett.119.108003)

Mass transport in nature and industrial processing takes place in nonequilibrium conditions under inhomogeneous concentration, stress, and temperature fields. Among these, the role of a temperature gradient is special because of the violation of the isothermal condition and the resulting strong out-of-equilibrium nature. For example, it is well known that migration of molecules takes place in a binary fluid under a temperature gradient: the so-called Ludwig–Soret effect [1]. This is a consequence of the balance between the mass flux and thermal flux in a steady state. Recently, this type of migration induced by a temperature gradient has been studied for soft materials such as polymer solutions, protein solutions, DNA solutions, colloidal suspensions, and liquid mixtures [2–17]. According to a simple consideration on the impact of a temperature gradient on Brownian motion, it is expected that migration takes place towards a low-temperature side, but many counter examples were reported (e.g., [6,13]), indicating the importance of considering all temperature-sensitive factors in a system.

However, all the above examples are the migration of discrete structures under a temperature gradient. It is interesting to consider how a temperature gradient affects the organization of soft continuous structures coexisting with a liquid, such as gels and membranes. Among such continuous structures, stacked membrane systems are particularly interesting since we can apply a temperature gradient along a specific direction, e.g., lateral or perpendicular directions.

Furthermore, in biological cells, transport of proteins and other molecules on membranes along the lateral direction plays an important role in biological functions. So far researches on lateral diffusion has been limited to that in an isothermal condition. It is interesting to study how inhomogeneous temperature fields affect such transport. However, before studying the lateral diffusion of proteins or molecules on a membrane, we should figure out the behavior of membranes themselves under a temperature gradient. Since a membrane is a continuous structure, it is not obvious how it reacts to inhomogeneous temperature fields.

In this Letter, we address this fundamental problem experimentally. To this end, we study a lamellar phase [18–21], or stacked membranes, of aqueous solution of nonionic surfactants, which is homeotropically aligned in between two parallel glass plates [22,23]. Since the lamellar order is stabilized by entropic repulsion known as the Helfrich interaction [18,20,24], it is expected that a temperature gradient has a significant impact on this phase. We find that membranes migrate under the constraint that the membrane topology, or the connectivity of each membrane, is to be preserved, resulting in the gradient of the degree of membrane fluctuations. We also show that we can induce motion of topological defects by a temperature gradient.

First we briefly explain our experiments (see [25] for the details). We use a mixture of surfactant molecules $C_{10}E_3$ and pure water. The surfactant molecules spontaneously form bilayers in water and then bilayers further form high

order structures such as lamellar and sponge phases (see Fig. S1 [25] for the phase diagram) [23,26]. The concentration of surfactants used are $\phi = 7$ wt% and 12 wt%. To measure the local surfactant concentration by fluorescence microscopy observation, we also put a small amount of fluorescent dye molecules, rhodamine 6G, which are almost perfectly attached to membranes [25]. We use two types of cells: the one is sandwiched by two parallel glass plates and the other is a wedge-shaped cell whose wedge angle $\theta = \tan^{-1}(0.01)$. We observe the behavior of the system under a temperature gradient by using the experimental setup shown in Fig. S2 [see also [25] for the details of the sample geometry and the temperature profile (Fig. S3)]. The temperature protocols used in our experiments are as follows. We first equilibrate our sample in the sponge phase at $T = 36^\circ\text{C}$ for 7 wt% and at $T = 38^\circ\text{C}$ for 12 wt%. The sponge phase is an isotropic disordered phase formed by bilayer membranes [18,21]. Then we cool the system with a very slow cooling rate of 0.01 K/min to 25°C for 7 wt% or 27°C for 12 wt%, in order to induce spontaneous formation of a homeotropically aligned lamellar phase, in which membranes are aligned in parallel to the glass substrates [27]. Then we anneal the sample over 24 hr. To apply a temperature gradient, we change the temperature of one of the two stages, while keeping the temperature of the other stage fixed. In the following, we refer to the regions on the high-temperature stage, between the two stages under the temperature gradient, and on the low-temperature stage as the HT, TG, and LT regions, respectively.

First, we investigate the time evolution of the fluorescence intensity $I(t)$ under a temperature gradient for the three (HT, TG, and LT) regions. The data in the HT (LT) regions are measured at 0.2 mm from the edges of the hotter (colder) stages. After preparation of the lamellar phase (see above), we heat the left stage from 27°C to 34°C with a heating rate of 1 K/min at $t = 0$ min, while keeping the right stage at 27°C . Since the lamellar phase is stable between 10°C and 36°C , the system keeps the homeotropically aligned lamellar order everywhere without transformation to the high-temperature sponge phase (see [25]). Figure 1(a) shows the temporal change in $I(t)$ between $t = 0$ min and $t = 1500$ min for the three regions. Here it should be noted that the fluorescent intensity is gradually decaying with time because of photobleaching effects induced by light exposure. We find that $I(t)/I(0)$ decays faster in the HT region than that in the LT region. In addition, $I(t)/I(0)$ slightly increases with time until $t = 250$ min in the LT region. As will be discussed later, these differences are not due to the temperature dependence of the fading rate of dyes. We also confirm that the decay rate of $I(t)$ is independent of the location and spatially homogeneous as long as the whole sample is in the same temperature.

Next we study the relaxation dynamics of the above system to a homogeneous temperature state after cooling only the left stage from 34°C to 27°C at $t = 1800$ min

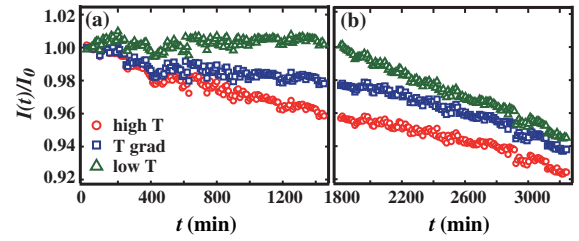


FIG. 1. (a) Temporal change in the fluorescence intensity $I(t)/I(0)$ for $\phi = 12$ wt% in the HT (circles), TG (squares), and LT (triangles) regions under the temperature gradient. (b) Temporal change of $I(t)/I(0)$ in the relaxation process to the equilibrium state at 27°C . After $t = 1800$ min under the temperature gradient, the temperature of the HT stage is set to the same as that of the LT stage.

with a cooling rate of 1 K/min to remove the temperature gradient. We note that there should be no temperature dependence of the fading rate in this relaxation dynamics because the temperature is homogeneous. We show in Fig. 1(b) the temporal change of $I(t)/I(0)$ after $t = 1800$ min, in order to see the difference in the decay rate among the three regions. We can see that the decay of $I(t)$ is slower in the HT region than in the LT region, which is the opposite of the response of the system to the temperature gradient described above.

Now we consider possible origins for the above described behaviors of the temporal change in the fluorescent intensity. There are four possibilities that come to our mind. (i) Temperature-gradient-induced change in the degree of membrane undulation fluctuations: larger membrane fluctuations in the LT region than in the HT region. A temperature gradient causes left-right imbalance of the strength of thermal force noise, resulting in a net lateral force on membranes towards the lower temperature direction. This leads to migration of membranes towards the LT side while accompanying the enhancement of out-of-plane membrane fluctuations. This allows the increase of the surfactant concentration in the LT side while keeping constant the number of membrane bilayers between the glass plates. We note that $I(t)$ is the integrated intensity over the sample thickness (z) direction. (ii) Larger membrane fluctuations at a lower local temperature: The amplitude of fluctuations decreases with an increase in temperature due to an unusual temperature dependence of the bending elasticity κ . Such anomalies were reported for some smectic lipid bilayer systems (see [28] and the references therein). (iii) Change in the lateral area of the surfactant molecules. The lateral area may be larger in the HT region than in the LT region since the tails of the surfactant molecules have more random configurations at a higher temperature. (iv) Increase in the number of the membranes in the LT region. However, possibilities (iii) and (iv) are less likely because of the following reasons: For (iii), the slow intensity change is not consistent with a quick response expected for the molecular-scale change of

the lateral area. For (iv), the increase of the number of membranes in a homeotropically aligned lamellar phase requires the formation of new edge dislocations, which is energetically too costly and not observed.

Hereafter we focus our attention on possibilities (i) and (ii) and check the validity of these scenarios experimentally. Under a homogeneous temperature gradient $|\nabla T|$ in the TG region, κ and the layer compression modulus B can be a function of T and/or $|\nabla T|$. Then we may generally express B at a position \vec{r} as $B(\vec{r}, T(\vec{r}), |\nabla T|)$. To clarify which of T or $|\nabla T|$ is essential for B , we introduce a new experimental method, focusing on the motion of edge dislocations in the lamellar phase confined in a wedge-shaped cell (see Ref. [22,29]). We note that in these experiments we do not put any dye molecules.

The basic idea behind this method is our expectation that the behavior of edge dislocations should be very sensitive to the degree of membrane undulation fluctuations, which is the origin of the layer compression modulus B . Note that the edge dislocation pattern is controlled by the competition between the elastic energy coming from the layer compression energy due to the deformation of smectic order imposed by the cell thickness gradient and that associated with the formation of edge dislocations: the formation of an edge dislocation can relax the layer compression energy by increasing the number of layers, while paying a cost of curvature elastic energy to bend the layers. Thus the equilibrium configuration is determined to minimize the sum of these two energy contributions. The distance between i th edge dislocation and $(i+1)$ th one from the tip of the wedge, λ_i , is determined by the energy associated with a layer spacing modulation, E_{layer} , and the energy cost for the edge dislocation formation, $E_{\text{edge}} = w \propto \kappa/d$, where d is the layer spacing (see, e.g., [22,29]). Then λ_i is given by

$$\lambda_i = \left(\frac{12w}{B \tan \theta} \right)^{1/3} s_i^{1/3}, \quad (1)$$

where θ is the wedge angle and s_i is the distance from the tip of the cell wedge to the i th edge dislocation. Then the position of the n th edge dislocation is $s_n = \sum_{i=0}^n \lambda_i$.

We show in Figs. 2(a)–2(c) the temporal change of the edge dislocation array at $\phi = 7\%$ in the TG region under a temperature gradient ($\nabla T \perp \vec{s}$): (a) $t = 0$ min, (b) $t = 300$ min, and (c) $t = 600$ min. Initially the system is equilibrated at 25°C . Then, the temperature of the left stage (the left edge in the images) is heated to 32°C at $t = 0$ min, while keeping the right stage at 25°C . We note that s is larger in the upper parts of Figs. 2(a)–2(c). The figure is a middle part of the sample from $s = 9.5$ to 10.5 mm. For visual aid, we highlight an edge dislocation by the yellow dotted line in each of Figs. 2(a)–2(c). Figure 2(d) shows the time evolution of the moving distance of the edge dislocation, Δs , from $t = 0$ min at two positions indicated by the left (circles) and right arrow

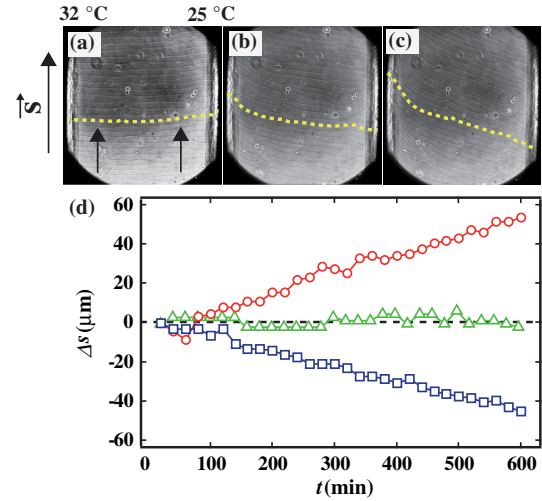


FIG. 2. Behavior of the edge dislocation array in a wedge-shaped cell under the temperature gradient ($\nabla T \perp \vec{s}$) for $\phi = 7$ wt%. We show phase contrast microscopy images at $t = 0$ min (a), 300 min (b), and 600 min (c) after heating the left stage from 25°C to 32°C while keeping the right stage at 25°C . The size of each image is 1×1 mm. The yellow dotted curves in (a)–(c) are drawn to follow the same edge dislocation line. See also Supplemental Material movie 1 [25], which shows the above process from 0 to 1200 min. (d) Temporal change of the y coordinate change of the defect line, Δs , caused by the temperature gradient. Circles and squares correspond to Δs at the locations pointed by the left and right arrows in image (a), respectively. For a reference, we also show Δs (open triangles) after homogeneously changing the temperature of the whole system from 25 to 32°C .

(squares) in Fig. 2(a). We also find that edge dislocations have larger moving distances s near the hotter (left) stage towards the positive s direction, whereas they move to the opposite direction near the colder (right) edge, despite that the temperature of the colder edge is unchanged. In addition, we confirm that edge dislocations do not move when we uniformly change the temperature from 25°C to 32°C [see open triangles in Fig. 2(d)]. This absence of edge dislocation motion suggests that the ratio κ/B is independent of T [see Eq. (1)]. Since the T dependences of κ and B would more likely go in opposite directions, our results indicate that these dependences should be weak. We can rule out possibility (ii) since it is due to the dependence of κ on a local temperature, for which we may assume local equilibrium. Accordingly, the only remaining possibility is scenario (i).

To further confirm this conclusion, we also investigate the phase-transition behavior from the lamellar phase to the sponge phase by heating the sample. First we apply a temperature gradient to a homeotropic lamellar phase for $t = 1440$ min and then we set both stages to the same temperature. Before the system is homogenized, we gradually heat the whole system homogeneously with a heating rate of 0.1 K/min. Then we observe that the transformation

of the lamellar phase to the sponge phase takes place earlier in the LT region. This phase transformation should more easily take place if the membranes have larger out-of-plane fluctuations. Thus, this result strongly indicates that the degree of membrane undulation fluctuations is indeed larger in the LT region than in the HT region, supporting scenario (i).

Now we discuss the reason why the membrane fluctuations become larger in the LT region under a temperature gradient, contrary to the equilibrium case. The membranes are very flexible and thermally fluctuating and the lamellar phase is stabilized by such thermal undulation fluctuations [24]. Here it is worth noting that our results show that the fluctuations become larger even for the LT region where $|\nabla T| = 0$. Under a temperature gradient, there should be a net thermal force acting on a membrane, which is exerted by liquid molecules, in the direction to the lower temperature, which transports the membrane towards the LT side under the constraint of the connectivity of each membrane, i.e., under the constant total number of membrane bilayers. This leads to excess surface area of membranes, resulting in the increase of out-of-plane membrane fluctuations in the LT region. Thus, the local layer compression modulus $B(\vec{r}, |\nabla T|)$ should be larger when \vec{r} is in the LT region, which is responsible for the tilting of the edge dislocations. We stress that this is a consequence of an integrated effect over the whole membranes in a nonequilibrium condition and not due to a local effect. The free energy of the lamellar phase is known to be proportional to $B/(\kappa d^3)$ in equilibrium. This indicates that the local free energy, or the chemical potential, is to be higher in the lower temperature. In a steady state under a temperature gradient, the osmotic force due to the chemical potential gradient should be balanced with the lateral force generated by the temperature gradient. However, the temperature affects not only membrane fluctuations, but also various intermolecular interactions in a complicated manner [4,11]. Thus we need further study to elucidate the temperature-gradient-induced migration mechanism unambiguously.

Next we show that we can control the edge dislocation spacing, λ , by applying a temperature gradient ∇T perpendicular to edge dislocations. The resulting changes in the edge dislocation pattern are shown in Figs. 3(a) and 3(b) when ∇T is in the same (setup A) and the opposite direction (setup B) to \vec{s} respectively. The figure is a middle part of the sample from $s = 9.5$ to 10.5 mm (see also Fig. S4 for the change of λ in the whole sample and the related discussion in [25]). Figures 3(c) and 3(d) show the temporal change in the locations of edge dislocations after heating the left stage from $T = 25^\circ\text{C}$ to 32°C . We find the response of λ is crucially dependent on the direction of ∇T : the opposite behavior is observed between setup A and B. We can see that λ increases (decreases) with time for setup A (see Supplemental Material movie 2 [25]) (setup B; see Supplemental Material movie 3 [25]). Figures 3(e) and 3(f) show the velocity v at $t = 200$ min as a function

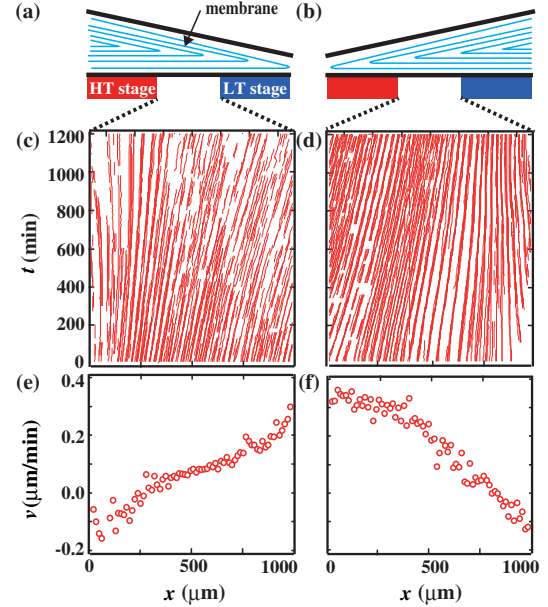


FIG. 3. Behavior of the edge dislocation array in a wedge-shaped cell for $\phi = 12$ wt% under the temperature gradient ($\nabla T/\bar{s}$) after heating the left stage from 25°C to 32°C at $t = 0$ min. We schematically show the cross sections of the system for two setups: (a) setup A and (b) setup B. (c) and (d) show trajectories of edge dislocations in the TG region for setup A and B, respectively. We can see that λ becomes broader (narrower) for setup A (setup B). See also Supplemental Material movies 2 and 3 [25], which show, respectively, the above processes of setup A and B from 0 to 1200 min. (e) and (f) show the x dependence of the line defect velocities, v , at $t = 200$ min for setup A and B, respectively. $\partial v/\partial x$ is positive (negative) for setup A (setup B).

of the x coordinate. We find that v increases (decreases) with an increase of the x coordinate for setup A (setup B). This is natural since the change of λ is equal to $\partial v/\partial x$. Here we note that the local equilibrium may be assumed thanks to the very slow motion of line defects.

Now we consider the physical mechanism of the above described behavior. As discussed above, an edge dislocation is formed by the competition between E_{layer} and E_{bend} . Under a temperature gradient, E_{layer} increases and E_{bend} decreases with an increase in the membrane undulation fluctuations. Thus, the edge dislocations migrate from the HT region to the LT region under the temperature gradient. The key is what portion of membranes are under the temperature gradient. An edge dislocation, a large portion of whose membranes is under the temperature gradient, moves more largely. Thus, edge dislocations with small s (or, near the tip of the wedge) is more strongly affected by the temperature gradient: v has a larger positive value for smaller s . For setup A, s is small near the LT stage, leading to $\partial v/\partial x > 0$. We note that v is slightly negative at $x < 100 \mu\text{m}$ for this setup. For setup B, on the other hand, s is small near the HT stage, leading to $\partial v/\partial x < 0$.

In summary, we study the out-of-equilibrium behavior of the homeotropic lamellar phase of bilayer membranes under a temperature gradient. Here we find that membrane undulation fluctuations become weaker at a higher T region, contrary to the equilibrium case, and explain this by the thermal force asymmetry acting on membranes caused by the temperature gradient. Furthermore, we show that edge dislocations can be manipulated by a temperature gradient. These intriguing features of the response of the lamellar phase to a temperature gradient originates from the connectivity of membranes. In our experiment, we were not able to reach a steady state under a temperature gradient since the process is too slow to follow because of a large size of our system (20 mm). It is quite interesting to study such a steady state since the connectivity should lead to an extra elastic force, which is to be balanced by a force induced by a temperature gradient and an osmotic force due to a concentration gradient. Our finding may open up a new avenue to control soft continuous structures and manipulate topological defects by a temperature gradient. We hope that our study provides an insight into material transport in biological systems induced by a temperature gradient.

This study was partly supported by Grants-in-Aids for Scientific Research (B) (17H02945), Young Scientists (A) (26707023), Scientific Research (S) (21224011) and Specially Promoted Research (25000002) from the Japan Society for the Promotion of Science (JSPS).

*kurita@tmu.ac.jp

†tanaka@iis.u-tokyo.ac.jp

- [1] S. de Groot and P. Mazur, *Non-Equilibrium Thermodynamics* (Dover Publications, New York, 1984).
- [2] R. Piazza and A. Guarino, *Phys. Rev. Lett.* **88**, 208302 (2002).
- [3] J. K. G. Dhont, *J. Chem. Phys.* **120**, 1632 (2004).
- [4] S. Wiegand, *J. Phys. Condens. Matter* **16**, R357 (2004).
- [5] R. Piazza, *J. Phys. Condens. Matter* **16**, S4195 (2004).
- [6] R. Kita, S. Wiegand, and J. Luettmer-Strathmann, *J. Chem. Phys.* **121**, 3874 (2004).
- [7] A. Onuki, *Phys. Rev. Lett.* **94**, 054501 (2005).
- [8] A. Onuki, *Phys. Rev. E* **75**, 036304 (2007).
- [9] S. Duhr and D. Braun, *Proc. Natl. Acad. Sci. U.S.A.* **103**, 19678 (2006).
- [10] H. Ning, R. Kita, H. Kriegs, J. Luettmer-Strathmann, and S. Wiegand, *J. Phys. Chem. B* **110**, 10746 (2006).
- [11] R. Piazza and A. Parola, *J. Phys. Condens. Matter* **20**, 153102 (2008).
- [12] M. Braibanti, D. Vigolo, and R. Piazza, *Phys. Rev. Lett.* **100**, 108303 (2008).
- [13] H.-R. Jiang, H. Wada, N. Yoshinaga, and M. Sano, *Phys. Rev. Lett.* **102**, 208301 (2009).
- [14] D. Vigolo, R. Rusconi, H. A. Stone, and R. Piazza, *Soft Matter* **6**, 3489 (2010).
- [15] Y. T. Maeda, A. Buguin, and A. Libchaber, *Phys. Rev. Lett.* **107**, 038301 (2011).
- [16] E. H. G. Backus, D. Bonn, S. Cantin, S. Roke, and M. Bonn, *J. Phys. Chem. B* **116**, 2703 (2012).
- [17] A. Würger, *Eur. Phys. J. E* **37**, 96 (2014).
- [18] M. Kleman and O. D. Lavrentovich, *Soft Matter Physics: An Introduction* (Springer, New York, 2003).
- [19] P. M. Chaikin and T. C. Lubensky, *Principles of Condensed Matter Physics* (Cambridge University Press, Cambridge, England, 1995).
- [20] S. A. Safran, *Statistical Thermodynamics of Surfaces, Interfaces, and Membranes* (Addison-Wesley, New York, 1994).
- [21] D. Roux, C. Coulon, and M. E. Cates, *J. Phys. Chem.* **96**, 4174 (1992).
- [22] F. Nallet and J. Prost, *Europhys. Lett.* **4**, 307 (1987).
- [23] Y. Iwashita and H. Tanaka, *Nat. Mater.* **5**, 147 (2006).
- [24] W. Helfrich, *Z. Naturforsch. Teil A* **33**, 305 (1978).
- [25] See Supplemental Material at <http://link.aps.org/supplemental/10.1103/PhysRevLett.119.108003> for the details.
- [26] T. D. Le, U. Olsson, K. Mortensen, J. Zipfel, and W. Richtering, *Langmuir* **17**, 999 (2001).
- [27] Y. Iwashita and H. Tanaka, *Phys. Rev. Lett.* **95**, 047801 (2005).
- [28] N. Chu and N. Kučerka, Y. Liu, S. Tristram-Nagle, and J. F. Nagle, *Phys. Rev. E* **71**, 041904 (2005).
- [29] Y. Iwashita and H. Tanaka, *Phys. Rev. E* **77**, 041706 (2008).